

Analytical and experimental characterisation of high-precision flexural pivots subjected to lateral loads

S. Zelenika^{a,*}, F. De Bona^b

^a Paul Scherrer Institut (PSI), Swiss Light Source (SLS), CH-5232 Villigen PSI, Switzerland

^b Università di Udine, Dipartimento di Ingegneria Elettrica, Gestionale e Meccanica, Via delle Scienze 208, I-33100 Udine, Italy

Received 31 May 2001; accepted 12 February 2002

Abstract

This work addresses the parasitic motion of high-precision rotation mechanisms based on flexural pivots subjected to lateral loads. This case has great importance from the mechanical design point of view, since generally flexural pivots support mechanical elements of considerable weight and their rotation is obtained by loading the pivot with a force instead of a pure couple.

From an analytical point of view, the problem is approached by studying the large deflections of an elastic frame. The equilibrium equations are considered and a solution based on the Newton–Raphson method is proposed. This approach is compared with other theoretical approaches. An experimental assessment performed by using laser interferometric techniques is presented. It is shown that the proposed solution allows the influence of lateral loads to be clearly established and proves to be adequate when the most common cases of limited lateral loads and rotations are considered.

© 2002 Elsevier Science Inc. All rights reserved.

Keywords: High-precision rotation; Flexural pivot; Geometrical non-linearities; Laser interferometry

1. Introduction

Flexural pivots (Fig. 1) are mechanical devices characterised by a high compliance with respect to the “in-plane” rotational degree of freedom (ϑ) and high stiffness in all other degrees of freedom. Usually such devices are referred to as cross-spring pivots, as they have a bi-symmetrical geometry and contain two leaf springs of equal dimensions crossing at their midpoints and forming an angle 2α . Generally, for stability, stiffness and ease of construction reasons, it is adopted $2\alpha = \pi/2$ [1].

Flexural pivots are commonly used in metrology as dynamometers and in seismometers, in pressure transducers, in the aerospace and motor fields, in optical instrumentation and in gyroscopes [2–11]. They are also used for several applications where particular working conditions (high or cryogenic temperatures, aggressive, dirty, ultra-clean and radiation environments [3,5,7,8,10–12]) do not allow conventional sliding and rolling bearings to be used. In these cases, the mechanical design of the pivots involves

the evaluation of the leaf springs strength and stiffness as well as a stability analysis of the overall mechanism [9,10,13].

Recently, such devices have also been used in precision engineering [11,12,14,15]. In fact, in flexural pivots the main sources of errors are systematic [1–3,5,6,9,16–18], since they are free from backlash, wear, stiction and friction—thereby resulting in a hysteresis that is generally well below 1% [13]. Hence, such drives permit a high rotational accuracy to be obtained via a rather simple, compact, reliable and maintenance-free design with limited production costs [11,19].

However, in high precision applications, a careful structural analysis has to be performed since, as shown in Fig. 1, the rotation ϑ is associated with a parasitic translation $\overline{OO'}$. As a consequence, the “geometrical” centre O of the pivot (which is defined as the intersection of the tangents to the elastic lines of the leaf springs at their movable joints and corresponds to the original centre of rotation of the pivot) moves to O'. This parasitic displacement, also termed centre-shift, can be characterised by establishing the variation of the amplitude d and the phase φ of the displacement $\overline{OO'}$, versus the rotation angle ϑ .

* Corresponding author. Tel.: +41-56-3104586; fax: +41-56-3103151.
E-mail address: sasa.zelenika@psi.ch (S. Zelenika).

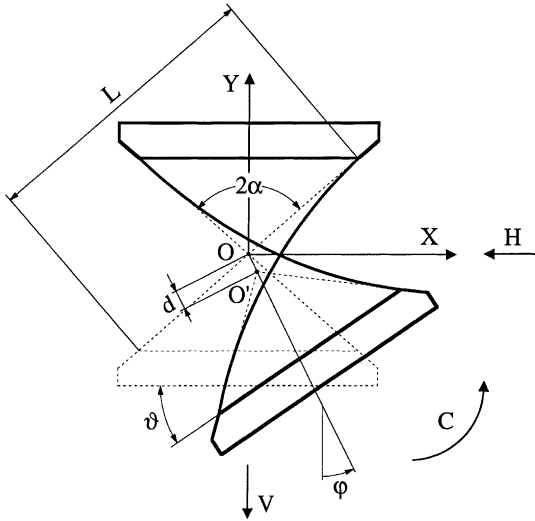


Fig. 1. Flexural pivot.

Several methods have been proposed in the literature to evaluate the parasitic motion OO' . In [20], the exact expression of the leaf spring curvature is used and a solution in terms of elliptic integrals is obtained for the case of the pivot loaded by a pure couple C . In this case the problem is symmetric and therefore the values of the reactions can be evaluated analytically. Other authors have obtained approximated solutions based on geometrical [7] or kinematic [18,21] considerations. However, all the above approaches do not account for the effects of the horizontal load H and of the vertical load V and yield results characterised by a wide scattering. The experimental results available in [1,17,21] do not make it possible to validate the reported theories, as the employed measurement techniques were characterised by a high uncertainty in the experimental techniques used (in fact, styluses, pointers or measuring and toolmakers' microscopes were used for the evaluation of the centre-shift [1,9,13,17,18]).

In this work an analytical method is presented that permits an evaluation of the parasitic motions even when the effects of the lateral loads H and V have to be considered. In order to establish the limits of applicability of the proposed method, an experimental assessment is then performed by using high-precision laser interferometric techniques.

2. Analytical model

The parasitic motion of the pivot can be evaluated following the approach suggested in [10]. In that case, however, the analysis was aimed mainly at the determination of the stiffness of the device in the vicinity of the undeflected position ($\vartheta = 0$), and therefore terms of the order smaller than ϑ^2 were neglected. In this work the overall working range of angular motions will be considered so that, even if the formalism given in [10] is followed, the assumptions of small

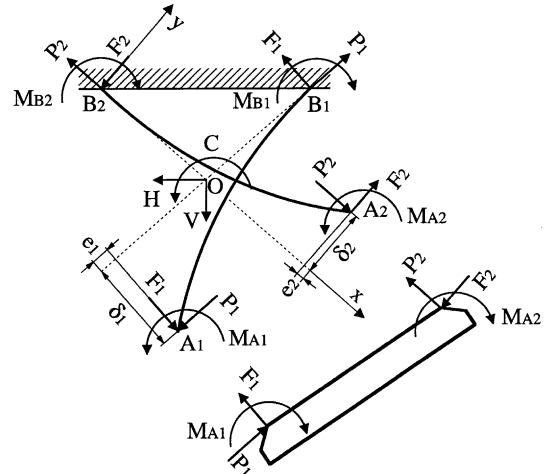


Fig. 2. Displacements and reactions.

deflections no longer hold and, taking into account the smaller order terms, the problem becomes strongly non-linear.

When the equilibrium conditions of a pivot in which the undeflected spring-strips cross at their midpoints are considered (Figs. 1 and 2), 11 variables define its behaviour: e_1 , e_2 , δ_1 , δ_2 , P_1 , P_2 , F_1 , F_2 , M_{B1} , M_{B2} and ϑ . A system of 11 equations is thus needed to solve the problem. Five of these are given by the equilibrium equations of the forces acting in the X and Y directions, the respective torque equilibrium, and the compatibility equations for the edges A_1 and A_2 of the leaf springs:

$$V = (P_1 + P_2)\cos \alpha + (F_1 - F_2)\sin \alpha \quad (1)$$

$$H = (P_1 - P_2)\sin \alpha - (F_1 + F_2)\cos \alpha \quad (2)$$

$$\begin{aligned} C &= M_{B1} - F_1 L \frac{1}{2} + M_{B2} - F_2 L \frac{1}{2} \\ &= M_{A1} + F_1 (L \frac{1}{2} - e_1) - P_1 \delta_1 + M_{A2} \\ &\quad + F_2 (L \frac{1}{2} - e_2) - P_2 \delta_2 \end{aligned} \quad (3)$$

$$\begin{aligned} (\delta_1 - \delta_2)\cos \alpha + (e_1 + e_2)\sin \alpha \\ = L \sin \alpha (1 - \cos \vartheta) \end{aligned} \quad (4)$$

$$(\delta_1 + \delta_2)\sin \alpha - (e_1 - e_2)\cos \alpha = L \sin \alpha \sin \vartheta \quad (5)$$

The remaining equations are obtained by considering the equilibrium of the single leaf springs, which can be addressed by following analytical approaches of different degrees of approximation. In fact, recently an analytical solution of the problem of large deflections of straight cantilever beams loaded at the free end by an axial force, where the exact expression of the leaf spring curvature is used (known as the *Elastica* [22]), was extended to the general case of loading [23], i.e., that of the spring-strips in Fig. 2. In this case the equilibrium equations of the spring-strips, assuming their mechanical characteristics (L , I , E) are identical, are:

$$EI \frac{d^2 y / dx^2}{[1 + (dy/dx)^2]^{3/2}} = P_{1(2)} y + M_{B1(2)} - F_{1(2)} x \quad (6)$$

where subscripts 1 and 2 refer respectively to leaf spring 1 and leaf spring 2, while x and y are the local Cartesian coordinate axes referred to the fixed edge of each spring-strip.

Again, as in [20], a solution in terms of elliptic integrals can be obtained. In this case, however, the computation can be addressed only through a lengthy iterative procedure with successive approximations [23]. Therefore, it seemed appropriate to pursue, in a first instance, the usage of the approximated expression for the curvature of the beam, where the influence of the axial load on the flexural behaviour of the beam is again taken into account, but for which, in the above curvature formula, the square of the derivative is neglected [9,10,20,22]. Eq. (6) therefore reduce to:

$$EI \frac{d^2y}{dx^2} = P_{1(2)}y + M_{B1(2)} - F_{1(2)}x \tag{6'}$$

It is worth noting here that expressing the elastic line in the form of Fourier series, as suggested in [22,24], does not allow the degree of uncertainty induced by the approximated expression for the curvature to be avoided, and implies an additional computational effort.

Eqs. (1)–(6') can now be written in dimensionless form by introducing the following notation [10]:

$$\begin{aligned} \lambda_{1(2)} &= \frac{e_{1(2)}}{\vartheta^2 L}, & \xi_{1(2)} &= \frac{2\delta_{1(2)}}{\vartheta L} - 1, \\ h &= \frac{HL^2}{EI} \operatorname{cosec} \alpha, & v &= \frac{VL^2}{EI} \sec \alpha, \\ f_{1(2)} &= \frac{F_{1(2)}L^2}{EI}, & 4\beta_{1(2)}^2 &= \frac{P_{1(2)}L^2}{EI}, \\ m_{B1(2)} &= \frac{M_{B1(2)}L}{EI} \end{aligned}$$

Integrating twice the expression (6') and imposing the corresponding boundary conditions, it follows:

$$f_{1(2)} = \vartheta \left(2\beta_{1(2)}^2 + 2\xi_{1(2)} \frac{\beta_{1(2)}^3}{\beta_{1(2)} - \tanh \beta_{1(2)}} \right) \tag{7}$$

$$m_{B1(2)} = \vartheta \left(\beta_{1(2)} \coth \beta_{1(2)} + \xi_{1(2)} \frac{\beta_{1(2)}^2 \tanh \beta_{1(2)}}{\beta_{1(2)} - \tanh \beta_{1(2)}} \right) \tag{8}$$

The expression for the in-axis deformation of the leaf spring, calculated considering the variation of its length from the initially straight form to the deformed shape in the equilibrium condition [10,22,24], is now used:

$$e_{1(2)} = \int_0^L \frac{1}{2} \left(\frac{dy}{dx} \right)^2 dx \tag{9}$$

By substituting Eq. (6') in (9) and integrating, it follows:

$$\lambda_{1(2)} = \frac{1}{16} \left(3 - \coth^2 \beta_{1(2)} + \frac{\coth \beta_{1(2)}}{\beta_{1(2)}} + 4\xi_{1(2)} \right) \tag{10}$$

The parameters $\lambda_1, \lambda_2, \xi_1$ and ξ_2 can now be expressed as functions of β_1 and β_2 . By substituting the expressions obtained into Eqs. (1) and (2), taking into account Eq. (7), and making the assumption that $2\alpha = \pi/2$, it is possible to write:

$$\begin{aligned} &4\beta_{1(2)}(4 + \vartheta^2)(\beta_{2(1)} \cosh \beta_{2(1)} - \sinh \beta_{2(1)}) \\ &\times \left[\frac{1}{2}(v \pm h) - 4\beta_{1(2)}^2 \right] \pm \beta_{2(1)}^2 \beta_{1(2)} \cosh \beta_{2(1)} \\ &\times \left\{ \beta_{2(1)} \left[\mp 32 + 16\vartheta + 16 \cos \vartheta (\pm 2 - \vartheta) \right. \right. \\ &+ 16 \sin \vartheta (2 \pm \vartheta) + \vartheta^2 \\ &\times \left(\mp 4 + 2\vartheta \pm \frac{4 \coth \beta_{1(2)}}{\beta_{1(2)}} \mp 2 \operatorname{cosech}^2 \beta_{1(2)} \right. \\ &\times (1 + \cosh 2\beta_{1(2)}) + \vartheta \operatorname{cosech}^2 \beta_{2(1)} \\ &\left. \left. \times (1 + \cosh 2\beta_{2(1)}) \right) \right] \\ &\left. - 2\vartheta [4 \tanh \beta_{2(1)}(4 + \vartheta^2) + \vartheta^2 \coth \beta_{2(1)}] \right\} = 0 \end{aligned} \tag{11}$$

These expressions hold if the leaf springs are under tensional loads; if compressive forces have to be considered, the parameter β becomes imaginary and therefore in Eq. (11) the substitution $\beta = i\omega$ (where $\omega = \sqrt{-PL^2/(4EI)}$) has to be introduced.

The derived non-linear system of equations with the variables β_1 and β_2 (ω_1 and ω_2 in the case of compression) as unknowns can be solved via a Newton–Raphson method. The calculation can be arranged according to an iterative approach: if V and H are known, v and h can also be evaluated; for a certain value of ϑ Eq. (11) is solved and the values of β_1 and β_2 are computed. The values of $\lambda_1, \lambda_2, \xi_1$ and ξ_2 , as well as of the deflections e_1, e_2, δ_1 and δ_2 can then be obtained. From Eqs. (7) and (8) the values of f_1, f_2 and of m_{B1}, m_{B2} can also be determined. Finally, by using Eq. (3), the value of the torque applied to the pivot can be calculated; this should then be compared with the actual value C . The procedure is repeated until convergence is reached.

Simple geometrical considerations finally allow the values of the displacements in the X and Y directions, and hence the amplitude and the phase of the centre-shift $\overline{OO'}$, to be obtained:

$$\frac{dX}{L} = \frac{\vartheta(\xi_1 + 1)}{2} \cos \alpha + \lambda_1 \vartheta^2 \sin \alpha + \frac{\sin(\alpha - \vartheta) - \sin \alpha}{2} \tag{12}$$

$$\frac{dY}{L} = \frac{\vartheta(\xi_1 + 1)}{2} \sin \alpha - \lambda_1 \vartheta^2 \cos \alpha - \frac{\cos(\alpha - \vartheta) - \cos \alpha}{2} \tag{13}$$

$$\frac{d}{L} = \sqrt{\left(\frac{d_X}{L}\right)^2 + \left(\frac{d_Y}{L}\right)^2}, \quad \varphi = \arctan\left(\frac{d_X/L}{d_Y/L}\right) \quad (14)$$

3. Experimental assessment

A cross-spring pivot with the following mechanical characteristics has been built: $L = 115$ mm, $t = 0.5$ mm—spring-strip thickness, $b = 15$ mm—spring-strip width, $\alpha = \pi/4$. The ratio b^2/t has been chosen so as to avoid the occurrence of anticlastic curvature even with the largest foreseen deflections [25], while a ratio $t/L \ll 1$ was adopted in order to minimise the effects induced by the compliance of the constraints and the hysteresis [13,17]. As suggested in [17], calibrated mounting jigs and gauges have been used to assure the equality of the lengths of the spring-strips and avoid their twisting during the assembly. The leaf springs have been clamped by using U-shaped clamping plates since these ensure a close contact at the front edge of the fixation, thus guaranteeing a uniform free working length of the strips [16]. The non-linearities caused by the mounting inaccuracies have been furthermore minimised by machining together both the clamping slits and the respective clamping parts.

The leaf springs were made of a beryllium–copper alloy ($E = 131$ GPa, $\sigma_R = 1,251$ MPa, $\sigma_{0.2} = 1,124$ MPa) as this material, of those suggested in the literature, has the largest figure of merit defined as the ratio $\sigma_{0.2}/E$ [26]; the other parts of the mechanism were made in AISI 304 steel. Following the approach suggested in [9,10], where a thorough analysis of the stability of the pivots was performed and the conditions when the pivot becomes unstable (i.e., when the restoring torques become negative) have been determined, the maximum working range of the angle $\vartheta (\pm\pi/6)$ and the values of the vertical load V (-70 N, $+12.5$ N) defining the stability range were established.

The measurement of the centre-shift $\overline{OO'}$ can be performed by considering the trajectory of the moveable block in the X – Y plane. This motion can be characterised by the values of the coordinates of a single point of the block versus the rotation angle ϑ .

An accurate measurement of the trajectory in three-dimensional space is generally performed by using laser tracking trilateration techniques [27–29]. In this way, the trajectory of a retroreflector connected to the moveable element is obtained from a measurement of the variation of its distance from three laser interferometers; the tracking of the retroreflector is obtained by using light-sensitive quadrant detectors.

In the case of flexural pivots, the laser tracking technique can be considerably simplified. In fact, only a two-dimensional measurement has to be performed; moreover, as the overall range of the amplitude d is limited, a suit-

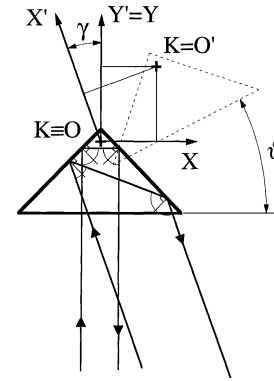


Fig. 3. Measurement principle.

able orientation of the retroreflector allows the centre-shift to be measured without reorienting the laser beams.

The measurement principle is schematically represented in Fig. 3. Two in-plane laser beams forming an angle γ are reflected by a corner cube whose optical centre K coincides with the geometrical centre of the pivot O . In order to achieve accurate measurements, the angle γ had to be carefully calibrated. For this purpose, a highly repeatable (± 0.1 μm) motion ψ was imposed to a linear stage bearing a goniometer (Fig. 4a). The imposed motion was measured with a single laser beam interferometer via a corner cube mounted on the goniometer. Varying the goniometer rotation, the maximum reading indicates the reached alignment of the direction of motion with the laser beam. The other laser beam is then used as well, and the goniometer is rotated towards the bisector of the angle defined by the two beams. The condition in which the readings along the two beam directions are identical and equal to a certain value χ allows the unknown angle to be determined as $\gamma = 2\arccos(\chi/\psi)$ (Fig. 4b). In this way it was established that $\gamma = 24^\circ 47'$.

Two single beam interferometers [19] therefore permit the components of the displacement $\overline{OO'}$ along X' and Y' to be measured and thus the values of d_X and d_Y to be determined. The correction of the displacement measurements versus the rotation angle ϑ due to the beam path in the rotated corner cube prism, which is made of glass and therefore has a different angle of refraction than air [30], was also taken into account (Fig. 5). Concurrently with the displacement measurements, the angle ϑ is measured by using a differential laser interferometric system [19].

Fig. 6 shows the set-up of the measurement system, which consists of a two frequency laser head, two single beam interferometers with their receivers, and a differential interferometer. The values of X' , Y' and ϑ were obtained by using a fringe counting board interfaced to a PC. The pivot can be loaded with couples and forces by means of a simple system based on calibrated weights connected by wires to the pivot centre. An increment of the loading was performed only when the system came to an

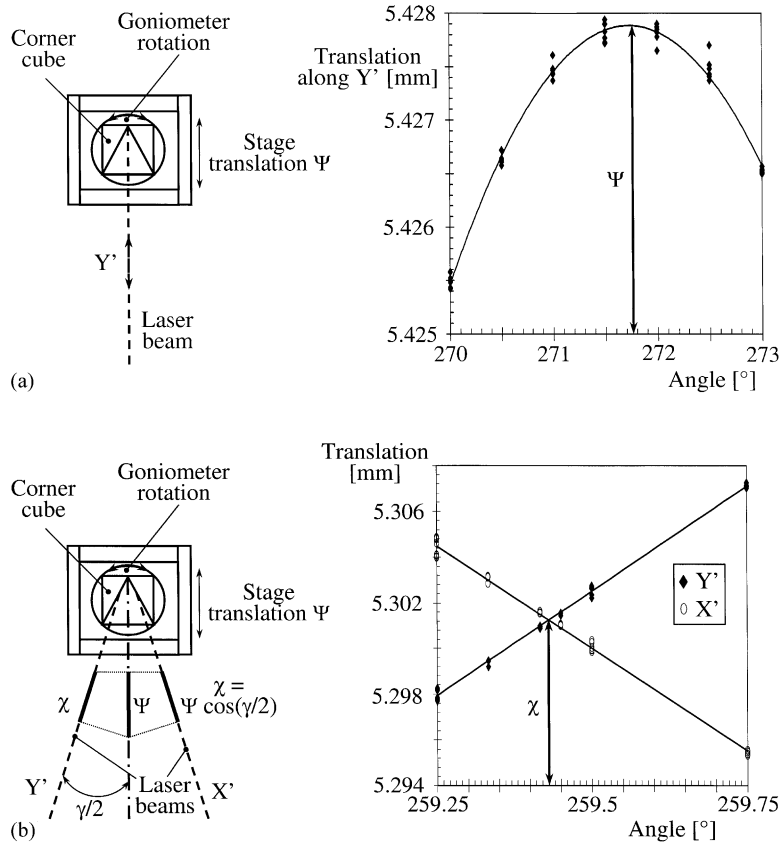


Fig. 4. Accurate evaluation of the angle γ between the two laser beams: alignment of the direction of motion with the laser beam along $Y' = Y$ (a) and determination of the bisector of the angle between the laser beams along X' and Y' (b).

almost complete rest since, due to known creeping effects associated with the adopted loading system, nanometric level motion is observed even after extended periods of time. At first the system was loaded by the single force V , and then the measurement was performed by increasing the applied torque and simultaneously measuring X' , Y' , and ϑ .

A resolution of 10 nm for linear displacements and of $0.2 \mu\text{rad}$ for angular displacements was achieved by using the illustrated measurement arrangement. The resulting interval of uncertainty is mainly due to systematic errors (alignment and assembly errors, uncertainty in the evaluation of γ); random errors (variation of the refractive index of air, dead-path error, etc. [19]) are negligible.

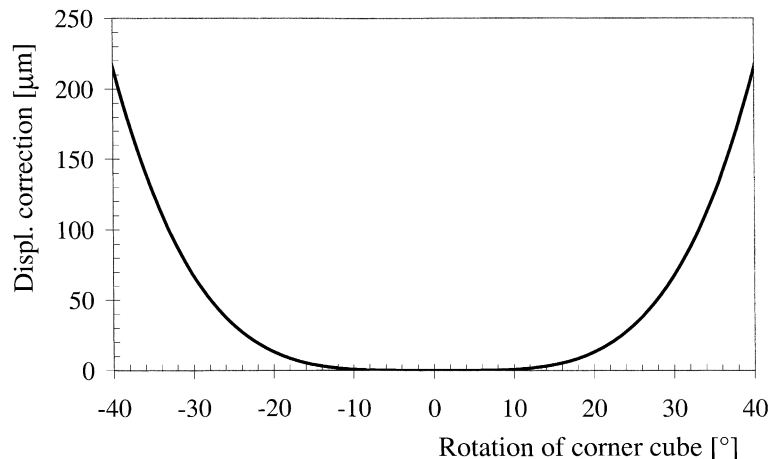


Fig. 5. Correction of the measured displacement due to the rotation of the corner cube.

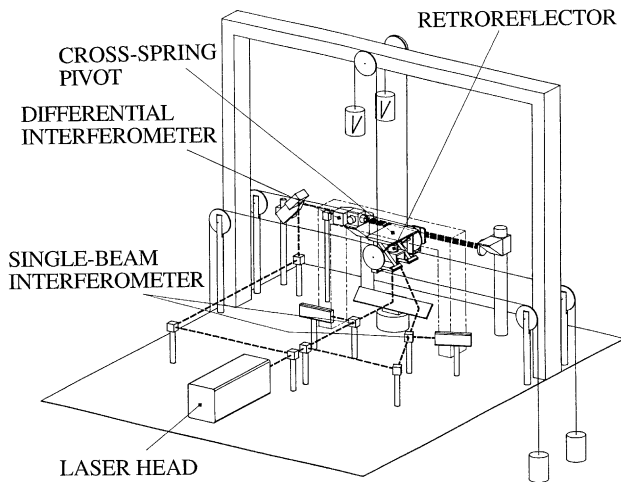


Fig. 6. Experimental set-up.

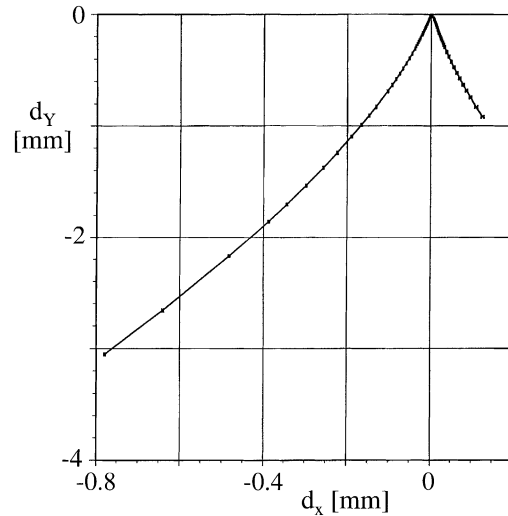


Fig. 7. Trajectory of the geometrical centre of the pivot.

4. Results and discussion

Fig. 7 shows the measured trajectory of the geometrical centre of the pivot in the X–Y plane for the case of a pivot loaded with a pure couple C ($V = H = 0$) whose value was gradually increased to 0.34 N m . The respective experimentally obtained dependence of the amplitude d and of the phase φ of the parasitic motion $\overline{OO'}$ on the angle ϑ , with the corresponding intervals of uncertainty, is then shown in Fig. 8. The measured values are compared here with the results obtained with the proposed analytical method, with those achieved by applying the analytical and the experimental methods available in the literature [1,7,17,18,20,21], as well as those obtainable with a simple geometric model of a rigid, hinged frame of equal geometry (geometric model).

The results can be compared more easily if the difference $\Delta d/L$ between the values of d/L obtained with the differ-

ent methods and those calculated with the method described in [20] is taken into account. In fact, in the case when the pivot does not undergo lateral loads, the solution proposed in [20], where the exact expression of the spring-strip curvature (Eq. (6)) is used, should be the most accurate. Therefore, in this particular case ($H = V = 0$), the values of $\Delta d/L$ correspond to the error introduced by the considered method.

In Fig. 8 it is noted that the results of the interferometric measurements are in excellent agreement with those obtained in [20]. The difference between the two methods is in fact smaller than 2% and this could be due to the residual compliance of the constrains. The method proposed in this work gives acceptable results, even if less accurate than those obtained in [7] and in [18]. This is due to the fact that the applicability of the adopted approximated expression for

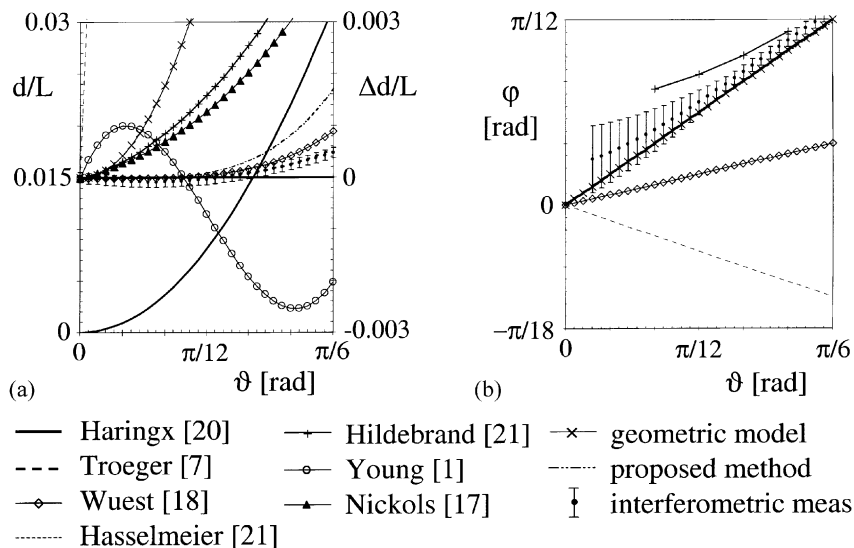


Fig. 8. The d/L , $\Delta d/L$ (a) and φ (b) versus ϑ in the case $V = H = 0$.

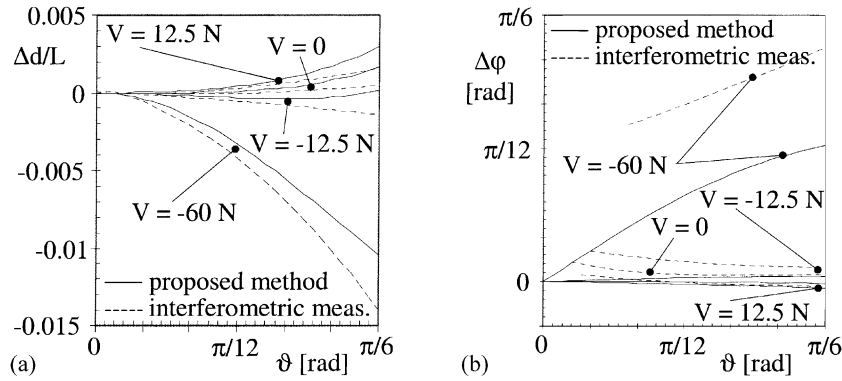


Fig. 9. The $\Delta d/L$ (a) and $\Delta\varphi$ (b) versus ϑ for different values of V .

the leaf spring curvature (Eq. (6')) is limited to smaller deflections.

When the phase φ is considered, it is evident that the proposed analytical method gives results similar to those reported in [7] and in [20] that are within the interval of uncertainty of the experimental measurements which, in this case, are not as accurate as for the amplitude. All the other methods result in very large errors, both in amplitude and in phase.

The validity of the analytical method proposed in this work is enhanced if the effect of the lateral loads is considered. In fact, since flexural pivots generally support mechanical elements characterised by considerable weight and their rotation is generally obtained by loading the pivot with a force instead of a pure couple, this case has great importance from the mechanical design point of view.

Fig. 9 shows the values of $\Delta d/L(\vartheta)$ and of $\Delta\varphi(\vartheta)$ (same meaning as $\Delta d/L$) obtained with the proposed analytical method as well as experimentally for different values of V . In these cases the intervals of uncertainty were not reported, but they are similar to those given in Fig. 8. The proposed method allows the influence of lateral loads to be clearly established. Only in the case of large rotations or when the values of V approach the instability conditions, the theoretical results become significantly different from those obtained experimentally. This behaviour can again be easily explained by considering that the approximated expression for the curvature used in Eq. (6') introduces errors that increase with increasing axial loads and leaf spring deflections [22]. It can be therefore concluded that the proposed method adequately describes the mechanical behaviour of the cross-spring pivot, if the difference between the approximated and the exact expression of the leaf spring curvature is limited.

5. Concluding remarks

The evaluation of the parasitic motion of a flexural pivot under lateral loads can be performed only if the non-linear behaviour of the leaf springs is considered. A first approach, suggested in this work, is to consider the equilibrium equa-

tions where the contribution of the axial loads is taken into account, but the approximated expression of the curvature is used. This approach gives an adequate solution if the most common cases of limited lateral loads and rotations are considered. A more accurate approach could be obtained by using the exact expression of the leaf spring curvature; this would, however, give rise to additional computational problems. In fact, in this case an expression in terms of elliptic integrals is obtained and hence in applying the Newton–Raphson method the Jacobian would have to be evaluated following lengthy numerical procedures [23]. Probably in the latter case the obtainable solution would not exhibit significant advantages with respect to an FEM approach.

The work on high-precision flexural pivots will continue by extending it to the case of pre-loaded leaf springs (i.e., springs deformed elastically during the pivot assembly) [31], as well as asymmetrical pivots (i.e., those where, for a given intersection angle of the strips, the point at which the undeflected strips cross is varied along their length) [10,21]. In fact, these configurations should decrease the variability of the rotational stiffness of the flexural pivot, thus reducing its centre-shift.

References

- [1] Young WE. An investigation of the cross-spring pivot. *J Appl Mech—ASME Trans* 1944;11:A113–A20.
- [2] Eastman FS. The design of flexure pivots. *J Aer Sci* 1937;16–21.
- [3] Olson JL. The evaluation of flexural pivots to meet critical performance and life requirements. *Des Eng Conf*, Chicago, USA, 1970.
- [4] Reiss RS. Fine adjustment for optical alignment. *Proc SPIE* 1986;608:63–9.
- [5] Seeling FA. Effectively using flexural pivots. *Des Eng Conf*, Chicago, USA, 1970.
- [6] Thorp AG II. Flexure pivots—design. *Prod Eng*, February, 1953;XXIV:192–200.
- [7] Troeger H. Considerations in the application of flexural pivots. *Aut Contr* 1962;17(4):41–6.
- [8] Weinstein WD. Flexure-pivot bearings—Part 1. *Mach Des*, June, 1965;150–7.
- [9] Wittrick WH. The theory of symmetrical crossed flexure pivots. *Aust J Sci Res* 1948;A1(2):121–34.

- [10] Wittrick WH. The properties of crossed flexure pivots and the influence of the point at which the strips cross. *Aer Quart* 1951;II:272–92.
- [11] URL: <http://www.lucasutica.com/pivots/>
- [12] Rundle WJ. Design and performance of an optical mount using cross-flexure pivots. *Proc SPIE* 1989;1167:306–12.
- [13] Siddall GJ. The design and performance of flexure pivots for instruments, MS Thesis. Department of Natural Philosophy, University of Aberdeen, Aberdeen, 1970.
- [14] Anderson EH, Moore DM, Fanson JL. Development of an active truss element for control of precision structures. *Opt Eng* 1990;29(11):1333–41.
- [15] Tabata M, Itoh N, Iye M. Active mirror support system for SUBARU telescope. *International progress in precision engineering*. London: Heinemann-Butterworths, 1993. p. 233–44.
- [16] National Physical Laboratory. Notes on Applied Science No. 15. London: H.M. Stat Off, 1956.
- [17] Nickols LW, Wunsch HL. Design characteristics of cross-spring pivots. *Engineering*, October, 1951;473–6.
- [18] Wuest W. Blattfedergelenke fuer Messgeraete. *Feinwerktechnik* 1950;54(7):167–70.
- [19] Slocum AH. *Precision machine design*. Englewood Cliffs: Prentice-Hall, 1992.
- [20] Haringx JA. The cross-spring pivot as a constructional element. *Appl Sci Res* 1949;A1(4):313–32.
- [21] Hildebrand S. Obliczanie i zachowanie sie w pracy sprzyn krzywiznowych. *Pomiary-Automatyka-Kontrola* 1958;11:501–8.
- [22] Timoshenko SP, Gere JM. *Theory of elastic stability*. 2nd ed. New York: McGraw-Hill, 1961.
- [23] De Bona F, Zelenika S. A generalized elastica-type approach to the analysis of large displacements of spring-strips. *Proc Inst Mech Eng C—J Mech Eng Sci* 1997;211:509–17.
- [24] Plainevaux JE. Guidage rectiligne sur lames elastiques. Comparison de divers types connus et nouveaux. *Il Nuovo Cimento* 1954;XII(1): 37–59.
- [25] Ashwell DG. The anticlastic curvature of rectangular beams and plates. *J R Aer Soc*, November, 1950;708–15.
- [26] Weinstein WD. Flexure-pivot bearings—Part 2. *Mach Des*, July, 1965;136–45.
- [27] Gilby JH, Parker GA. Laser-tracking system to measure robot arm performance. *Sens Rev*, October, 1982;180–4.
- [28] Jiang BC, Black JT, Duraisamy R. A review of recent developments in robot metrology. *Manuf Syst* 7(4);339–57.
- [29] Nakamura O, Goto M. Laser interferometric calibration of microscan mechanisms by using three laser beams. *Precision Eng* 1993;15(1): 39–43.
- [30] Peck ER. Theory of the corner-cube interferometer. *J Opt Soc Am* 1948;38(12):1015–24.
- [31] Hildebrand S. Zur Berechnung von Torsionbaendern im Feinge-raetebau. *Feinwerktechnik* 1957;61(6):191–8.